J. Chem. Sci. Vol. 127, No. 4, April 2015, pp. 609–618.
DOI 10.1007/s12039-015-0815-0

Polypyridyl iron(II) complexes showing remarkable photocytotoxicity in visible light

ADITYA GARAI[a], UTTARA BASU[a], ILA PANT[b], PATURU KONDAIAH[b,*] and AKHIL R CHAKRAVARTY[a,*]

[a]Department of Inorganic and Physical Chemistry, Indian Institute of Science, Bangalore 560012, India
[b]Department of Molecular Reproduction, Development and Genetics, Indian Institute of Science, Bangalore 560012, India
e-mail: paturu@mrdg.iisc.ernet.in; arc@ipc.iisc.ernet.in

MS received 11 October 2014; revised 17 November 2014; accepted 22 November 2014

Abstract. Iron(II) complexes of polypyridyl ligands (B), *viz.* $[Fe(B)_2]Cl_2$ (**1** and **2**) of *N*, *N*, *N*-donor 2-(2-pyridyl)-1,10-phenanthroline (pyphen in **1**) and 3-(pyridin-2-yl)dipyrido[3,2-a:2',3'-c]phenazine (pydppz in **2**), are prepared and characterized. They are 1:2 electrolytes in aqueous DMF. The diamagnetic complexes exhibit metal to ligand charge transfer band near 570 nm in DMF. The complexes are avid binders to calf thymus DNA giving binding constant (K_b) values of $\sim 10^6$ M^{-1} suggesting significant intercalative DNA binding of the complexes due to presence of planar phenanthroline bases. Complex **2** exhibits significant photocytotoxicity in immortalized human keratinocyte cells HaCaT and breast cancer cell line MCF-7 giving IC_{50} values of 0.08 and 13 μM in visible light (400–700 nm). Complex **2** shows only minor dark toxicity in HaCaT cells but is non-toxic in dark in MCF-7 cancer cells. The light-induced cellular damage follows apoptotic pathway on generation of reactive oxygen species as evidenced from the dichlorofluorescein diacetate (DCFDA) assay.

Keywords. Iron; polypyridyl bases; DNA binding; photocytotoxicity; apoptosis.

1. Introduction

Photodynamic therapy (PDT) involves selective targeting and damaging cancer cells leaving unexposed healthy cells unaffected by photo-activating a drug in the tumour cells with visible or near IR light.[1–5] Porphyrins and phthalocyanines are extensively studied for their photocytotoxic activity resulting from generation of singlet oxygen ($^1O_2$) as the reactive oxygen species (ROS) in a type-II energy transfer pathway involving the $^3(\pi–\pi^*)$ state of the drug and molecular oxygen in its triplet ground state ($^3O_2$).[6,7] The efficacy of these PDT agents depends primarily on the quantum yield of singlet oxygen generation and Photofrin® is currently known as the FDA approved PDT drug. The porphyrin bases generally show skin photosensitivity and hepatotoxicity thus significantly limiting their therapeutic potential.[8,9] These predicaments have generated interests to develop the chemistry of metal-based PDT agents as suitable alternatives to Photofrin.[10–20] Metal complexes could show photocytotoxicity via different mechanistic pathways that include type-I and/or photo-redox pathway forming superoxide or hydroxyl radicals as the ROS besides having the type-II $^1O_2$ pathway.[7] We have recently reported iron(III) and oxovanadium(IV) complexes as potential 3d metal-based PDT agents displaying significant light-induced cytotoxicity.[21–23] Metal-based PDT agents are thus emerging as new generation anti-cancer agents along with several recent advancements on platinum based chemotherapeutic and photo-chemotherapeutic agents.[24–26] The present work stems from our interests to develop iron-based photocytotoxic agents considering the bio-essential nature of iron and its important redox and photophysical chemistry. Bleomycins (BLMs) are the iron-based natural anti-tumour agents which show oxidative damage of DNA in cancer cells forming cytotoxic hydroxyl radicals.[27,28]

Iron complexes with the metal in its +3 oxidation state are prone to reduction inside the cells by cellular reducing agents like glutathione (GSH). Iron(III) complexes having azide ligand are known to show significant DNA photocleavage activity.[29] We have reported a high spin (S=5/2) ternary iron(III) complex [Fe(BHA)(L)Cl] of a dipicolylamine derivative (L) and benzhydroxamic acid (HBHA) which shows photocytotoxicity giving an IC_{50} value of 14.6 μM upon irradiation with a visible light (400–700 nm) in HeLa cancer cells.[30] The iron(III) complexes are susceptible to show undesired chemical nuclease activity due to *in situ*

*For correspondence

generation of reactive iron(II) species by GSH. In contrast, the metal in its stable diamagnetic +2 oxidation state is expected to have low dark toxicity. We have thus designed low-spin iron(II) complexes as a new class of photocytotoxic agents in visible light using polypyridyl ligands that could stabilize the metal in its lower oxidation state. There are few reports on iron(II) complexes modelling the biological activity of bleomycins (BLMs).[31–34] High spin (S=2) iron(II) complexes having pentadentate polypyridyl ligands are known to show cytotoxicity in dark giving IC_{50} values of 1.1 to 7.7 μM in various cancer cell lines.[31] The iron(II) complexes showing the BLM activity are generally not suitable for PDT application as the primary requirement of a PDT agent is that the complex must be less or non-toxic in dark while being highly photocytotoxic in visible light. Keeping that in mind, we have prepared two iron(II) complexes, viz. $[Fe(B)_2]Cl_2$ (**1** and **2**) of *N*, *N*, *N*-donor 2-(2-pyridyl)-1,10-phenanthroline (pyphen in **1**) and 3-(pyridin-2-yl)dipyrido[3,2-a:2',3'-c]phenazine (pydppz in **2**) and the complexes show significant photo-induced cytotoxicity in immortal human keratinocyte cell line HaCaT and breast cancer cell line MCF-7 (figure 1).

2. Experimental

2.1 *Materials and methods*

All the reagents and chemicals were procured from commercial sources (SD Fine Chemicals, India; Aldrich, USA) and used without any further purification. Solvents used were purified by standard procedures.[35] Calf thymus (ct) DNA, ethidium bromide (EB), Hoechst 33258, 2',7'-dichlorofluoresceindiacetate (DCFDA), 3-(4,5-dimethylthiazol-2-yl)-2,5-diphenyltetrazolium bromide (MTT), propidium iodide (PI), acridine orange (AO), Dulbecco's modified eagle medium (DMEM), Dulbecco's phosphate buffered saline (DPBS) and fetal bovine serum (FBS) were purchased from Sigma, USA. Tris-(hydroxymethyl)aminomethane-HCl (Tris-HCl) buffer solution was prepared using deionized and sonicated triple distilled water using a quartz water distillation setup. The *N*, *N*, *N*-donor heterocyclic bases 2-(2-pyridyl)-1,10-phenanthroline (pyphen) and 3-(pyridin-2-yl)dipyrido[3,2-a:2',3'-c]phenazine (pydppz) were prepared following literature procedures.[36–38]

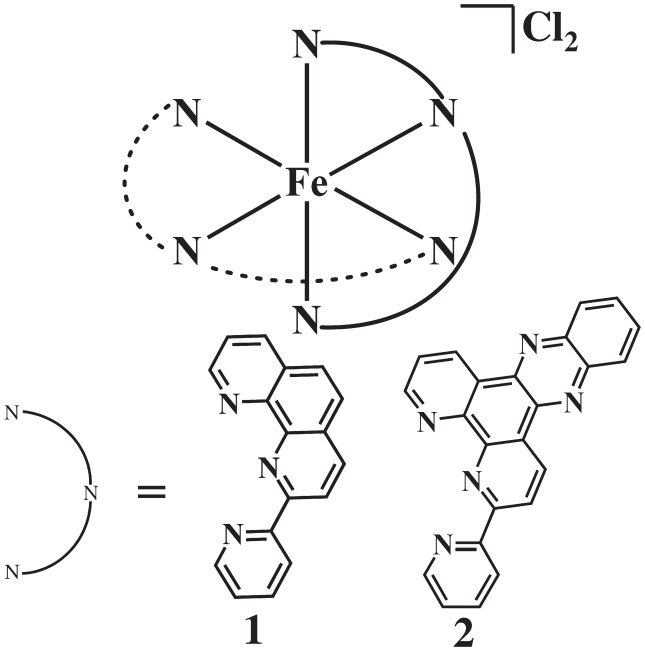

Figure 1. Schematic representation of the polypyridyl bases and complexes **1** and **2**.

The elemental analyses were done using a Thermo Finnigan Flash EA 1112 CHNS analyzer. The infrared spectra were recorded on a Bruker ALPHA FT-IR spectrometer. Electronic spectra were obtained on a Perkin-Elmer Lambda 650 spectrophotometer. Molar conductivity measurements were carried out using a Control Dynamics (India) conductivity meter. Electrospray ionization mass spectra (ESI-MS) were recorded using Bruker Daltonics make Esquire 300 Plus ESI Model. ^{1}H NMR spectra were recorded at room temperature on a Bruker 400 MHz NMR spectrometer. Flow cytometry (FACS) measurements were done using Calibur (Becton Dickinson (BD) cell analyzer) at FL1 channel. Imaging studies were done with Zeiss LSM510 apochromat confocal laser scanning microscope.

2.2 *Synthesis of the complexes*

Complexes **1** and **2** were prepared by following a general synthetic procedure in which a methanol solution (25 mL) of the respective base (0.514 g, pyphen; 0.718 g, pydppz; 2.0 mmol) was added dropwise to a methanol solution (25 mL) of $FeCl_2$ (0.125 g; 1.0 mmol). Stirring of the reaction mixture for 30 min gave a deep purple coloured solution. The solvent was evaporated and the residue was washed with cold ethanol followed by cold diethyl ether, and finally dried in vacuum over P_4O_{10}.The characterization data for the complexes are given below.

2.2a *[Fe(pyphen)$_2$]Cl$_2$(**1**)*: [Yield: 0.54 g, 85%] Analysis: Calculated for $C_{34}H_{22}Cl_2FeN_6$: C, 63.68; H, 3.46; N, 13.10. Found: C, 63.53; H, 3.62; N, 12.98. ESI-MS in 10% aqueous MeOH: *m*/*z*285.42 $[M\text{-}2Cl]^{2+}$. IR / cm^{-1}: 2960w, 2911w, 1735w, 1607m, 1440vs, 1382vs,

1254s, 1195w,1100m, 1000m, 843vs,730m, (vs, very strong; s, strong; m, medium; w, weak). UV-visible in DMF [λ_{max}/nm (ε/ M^{-1} cm^{-1})]: 580 (5200), 484sh (4490), 347 (17290), 304 (34440) (sh, shoulder). Conductivity in 20% aqueous DMF (Λ_M): 145 S cm^2M^{-1}.

2.2b *[Fe(pydppz)$_2$]Cl$_2$(**2**)*: [Yield: 0.76 g, 90%] Analysis: Calculated for $C_{46}H_{26}Cl_2FeN_{10}$: C, 65.34; H, 3.10; N, 16.57. Found: C, 65.67; H, 3.31; N, 16.55. ESI-MS in 10% aqueous MeOH: m/z387.63 $[M\text{-}2Cl]^{2+}$. IR / cm^{-1}: 3045w, 2912w, 1607s, 1539w, 1480w, 1401s, 1343vs, 1254m, 1118m, 1041m, 725s, 590w. UV-visible in DMF [λ_{max}/nm (ε/ M^{-1} cm^{-1})]: 556 (4250), 388sh (20740), 367 (30690), 289 (62320). Conductivity in 20% aqueous DMF (Λ_M): 142 S cm^2M^{-1}.

2.3 *Theoretical studies*

The geometry of the complexes **1** and **2** was optimized by density functional theory (DFT) method using B3LYP/LanLD2Z level as implemented in Gaussian 09 program. The electronic transitions with their transition probability were obtained using linear response time dependent density functional theory (TDDFT).

2.4 *DNA binding*

DNA binding experiments were done in Tris-HCl/NaCl buffer (5 mM Tris-HCl, 5 mM NaCl, pH 7.2) using DMF solution of the complexes **1** and **2**. Calf thymus (ct) DNA (ca. 250 μM NP) in the buffer medium gave a UV absorbance ratio of ca. 1.9:1 at 260 and 280 nm indicating that the DNA is apparently free from any protein impurity. The concentration of ct-DNA was estimated from its absorption intensity at 260 nm with a known molar extinction coefficient value (ε) of 6600 $M^{-1}cm^{-1}$.[39] The absorption titration experiments were done by procedures as described.[6] The intrinsic equilibrium binding constant (K_b) and the MvH equation fitting parameter (s) of **1** and **2** to ct-DNA were obtained by McGhee-von Hippel (MvH) method using the expression of Bard and co-workers by monitoring the change of the absorption intensity of the spectral bands with increasing concentration of ct-DNA.[40,41]

DNA melting experiments were carried out by monitoring the absorbance of ct-DNA (200 μM) at 260 nm at various temperatures, both in the absence and presence of the complexes (25 μM). Measurements were carried out using a Perkin-Elmer Lambda 650 spectrometer with a temperature controller at an increase rate of 0.5°C per min of the solution. Ethidium bromide (EB) was used as a control. Viscometric titrations were performed with a Schott Gerate AVS 310 automated viscometer that was maintained at 37°C in a constant temperature bath. The concentration of ct-DNA was 150 μM in NP (nucleotide pair) and the flow times were measured using an automated timer. Each sample was measured 3 times and an average flow time was calculated. Data were presented as $(\eta/\eta_0)^{1/3}$ *vs.* [complex]/[DNA], where η is the viscosity of DNA in the presence of complex and η_0 is that of DNA alone. Viscosity values were calculated from the observed flow time of DNA-containing solutions (t) corrected for that of the buffer alone (t_0), $\eta = (t - t_0)/t_0$. Due corrections were made for the viscosity of DMF solvent present in the solution.

2.5 *Cytotoxicity measurements by MTT assay*

The cytotoxicity of the complexes was studied using MTT assay in light and dark. This method is based on the ability of mitochondrial dehydrogenases of viable cells to cleave the tetrazolium rings of MTT, forming dark purple membrane impermeable crystals of formazan that can be estimated from the spectral measurements in DMSO.[42] Approximately, 8000 cells (human immortalized keratinocytes HaCaT cells and breast cancer MCF-7cell line) were plated separately in a 96 wells culture plate in Dulbecco's Modified Eagle Medium (DMEM) containing 10% FBS. After 24 h of incubation at 37°C in 5% CO_2 atmosphere, various concentrations of the complexes dissolved in 1% DMSO were added to the cells, and incubation was continued for 4 h in dark. The media was subsequently replaced with DPBS and irradiated with a broad band visible light (400−700 nm, 10 J cm^{-2}), using a Luzchem Photoreactor (Model LZC-1, Ontario, Canada). After irradiation, DPBS was removed and replaced with DMEM/FBS, and incubation was continued for a further period of 20 h in dark. After the incubation period, 5 mg mL^{-1} of MTT (20 μL) was added to each well and incubation continued for an additional 3 h. The culture medium was discarded and 200 μL of DMSO was added to dissolve the formazan crystals. The absorbance was measured at 540 nm using a Molecular Devices Spectra Max M5 plate reader. Cytotoxicity of the complexes was measured as the percentage ratio of the absorbance of the treated cells to the untreated controls. The IC_{50} values were determined by nonlinear regression analysis (GraphPad Prism 5).

2.6 *DCFDA assay for ROS generation*

DCFDA was used to detect the generation of any cellular ROS.[43] Cell permeable DCFDA can be oxidized by cellular ROS to generate fluorescent 2′, 7′-dichlo-

rofluorescein (DCF) with an emission maxima at 525 nm.[44] MCF-7 cells were incubated with the complexes **1** (60 μM) and **2** (5 μM) for 4 h followed by irradiation with visible light (400−700 nm) for 1 h in DPBS. Cells treated with complexes **1** and **2** in dark were used as controls. The cells were harvested by trypsinization and washed with DPBS. A single cell suspension of 1×10^6 cells per mL was made and treated with 1 μM DCFDA solution in dark for 15−20 min at 25°C. The distribution of DCFDA stained MCF-7 cells was determined by flow cytometry in the FL-1 channel.

2.7 *Cell cycle analysis*

To investigate the effect of the complexes on the cell cycle, 3×10^6MCF-7 cells were plated per well of a 6 wells tissue culture plate in DMEM containing 10% FBS. After 24 h of incubation at 37°C in a CO_2 incubator, DMSO solutions of the complexes **1** (60 μM) and **2** (5 μM) were added to the cells, and incubation was continued in dark for 4 h. The medium was subsequently replaced with DPBS, and photo-irradiation was done with visible light of 400−700 nm using the Luzchem photoreactor for 1 h. After irradiation, DPBS was removed and replaced with DMEM containing 10% FBS, and incubation was continued in the dark for a further period of 24 h. Cells were then trypsinized and collected into 1.5 mL centrifuge tubes. The cells were washed once with DPBS (pH = 7.4) and fixed by adding 800 μL of chilled 70% methanol dropwise with constant and gentle vortexing to prevent any cell aggregation. The cell suspensions were incubated at 20°C for 6 h. The fixed cells were then washed twice with 1.0 mL of DPBS by centrifuging at 4000 rpm at 4°C for 5 min. The supernatants were gently discarded, and the cell pellets were suspended in 200 μL of DPBS containing 10 mM mL^{-1} DNasefree RNase at 37°C for 12 h. After digestion of cellular RNA, a 20 μL volume of 1.0 mg mL^{-1} propidium iodide (PI) solution was added to both the mixtures, which were incubated at 25°C in the dark for another 20 min. Flow cytometric analysis was performed using a FACS Calibur Becton Dickinson (BD) cell analyzer at FL2 channel (595 nm), and the distribution of cells in various cell cycle phases was determined from the histogram generated by Cell Quest Pro software (BD Biosciences). Data analysis for the percentage of cells in each cell cycle phase was performed by using WinMDI version 2.8.

2.8 *Ethidium bromide/acridine orange dual staining*

The changes in chromatin organization in MCF-7 cells after photo-irradiation were determined after treatment with complexes **1** (60 μM) and **2** (5 μM) by dual staining method using acridine orange (AO) and ethidium bromide (EB). About 2×10^4 cells were allowed to adhere overnight on a coverslip placed in each well of a 12 well plate. The cells were treated with the complex for 4 h in the dark, followed by irradiation with visible light of 400–700 nm (10 J cm^{-2}). Dark controls were also used. The cells were then allowed to recover for 1 h, washed with DPBS, stained with AO/EB mixture (1:1, 10 μM) for 15 min. The cover slips were mounted using antifade and observed with a confocal laser scanning microscope (Zeiss LSM 510 apochromat).

3. Results and Discussion

3.1 *Synthesis and characterization*

Iron(II) complexes $[Fe(B)_2]Cl_2$ (**1** and **2**) of two tridentate polypyridyl bases (B), *viz*. 2-(2-pyridyl)-1,10-phenanthroline (pyphen) in **1** and 3-(pyridin-2-yl)dipyrido[3,2-a:2',3'-c]phenazine (pydppz) in **2** were prepared by a general synthetic procedure in which one equivalent of $FeCl_2$ was reacted with two equivalents of the corresponding base in methanol (figure 1). The complexes were characterized from the analytical and spectral data. Selected physicochemical data are given in table 1. Both the complexes showed good solubility in DMF, DMSO, dichloromethane and chloroform. They were moderately soluble in methanol, ethanol and acetonitrile. The complexes were found to be stable in both solid and solution phases as seen from the UV-visible absorption spectral data which remained unaltered for a period of 24 h. The ESI-MS spectra of the complexes in aqueous methanol showed a single prominent peak corresponding to the molecular ion peak $[M-2Cl]^{2+}$. The molar conductivity data showed that the complexes are 1:2 electrolytic in aqueous DMF (∼145 S cm^2M^{-1}). The electronic absorption spectra of the complexes in DMF showed a metal to ligand charge transfer (MLCT) transition near 580 nm. Ligand centred $\pi \rightarrow \pi^*$ transition bands were observed near 280 nm (figure 2). The pydppz complex displayed two additional bands at 390 nm and 367 nm assignable to the $n \rightarrow \pi^*$ transitions of the phenazine moiety.[45] The complexes are redox active showing cyclic voltametric responses involving the metal centre and the polypyridyl bases in DMF *vs.* SCE using 0.1 M TBAP as the supporting electrolyte. Both the complexes show oxidative response near 1.0 V corresponding to the Fe(III)-Fe(II) couple. Quasi-reversible redox responses were observed at −1.08 V for **1** and −0.8, −1.13 V for **2** corresponding to the polypyridyl base.

Table 1. Physicochemical data and DNA binding parameters for the complexes **1** and **2**.

Complex	λ(nm) (ε / M^{-1} cm^{-1})[a]	Λ_M^b(S cm^2M^{-1})	E^c(V)	K_b^d x10^{-6} (M^{-1})[s]	ΔT_m^e(°C)
1	580(5200)	145	1.01	1.1 (±0.3) [0.4]	1.0
2	556(4250)	142	1.0	3.4 (±0.6) [0.6]	2.7

[a]In DMF. [b]Molar conductivity value in 20% aqueous DMF at 25°C. [c]Potential vs. SCE in DMF -0.1 M TBAP at a scan rate of 50 mV s^{-1}. [d]Intrinsic binding constant to ct-DNA (MvH eq. fitting parameter) with 10 μM complex concentration. [e]Change in the ct-DNA melting temperature in phosphate buffer (pH = 6.8).

3.2 *Theoretical study*

Theoretical calculations were carried out using B3LYP level of DFT (density functional theory) to understand the photophysical and redox properties of the complexes (figure 3).[46–49] Following the orbital arguments proposed by Amouyal and co-workers, calculations were performed on geometrically modified iron(II) complexes. As expected, considerable d-orbital contribution from the iron was observed in the HOMO and LUMO is found to be localized on the polypyridyl ligand. MLCT having high oscillator strength was found to be operative in both the complexes. The electronic transitions tallied with the theoretical assignments performed using TDDFT calculations.

3.3 *DNA binding studies*

Absorption spectral titration was used to monitor the mode of interaction of the complexes **1** and **2** with ct-DNA (figure 4). The intrinsic equilibrium DNA binding constant (K_b) values of the complexes are given in table 1. The K_b values of $\sim 10^6 M^{-1}$ follow the order: **2** > **1**. The pydppz complex **2** with an extended planar aromatic moiety showed higher DNA binding strength than the pyphen analogue **1**.[50] This is in accordance with the recently reported result that extended planarity gives better ability to bind the DNA double helix.[51] The K_b values indicate partial intercalative DNA binding nature of the complexes.

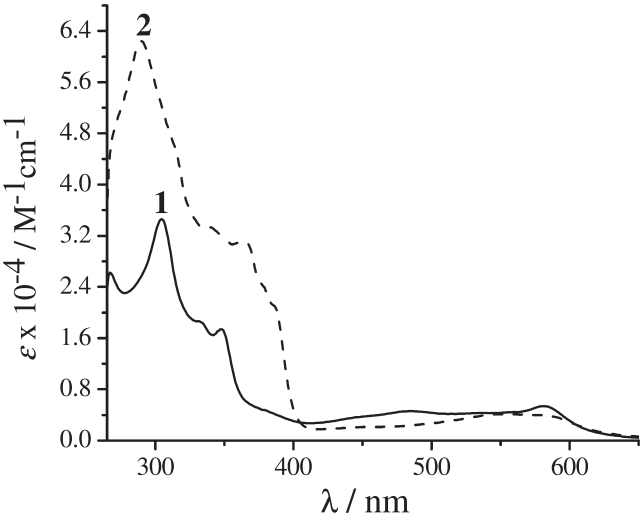

Figure 2. Electronic absorption spectra of the complexes **1** (—) and **2** (- - -) in DMF.

Thermal denaturation experiments were done to gain insight into the stability of the DNA double helix upon binding to **1** and **2** (figure 5a). A small positive shift of the DNA melting temperature (ΔT_m) was observed upon addition of complex **1** to ct-DNA. The moderate ΔT_m value suggests primarily groove binding nature of the complex to ct-DNA in preference to an intercalative mode of binding that normally results in large positive ΔT_m value.[52,53] The ΔT_mvalue for the pydppz complex **2** is higher than that of the pyphen complex **1**. It is apparent from the data that the extended aromatic rings are involved in the binding to ct-DNA. Viscosity measurements were carried out to examine the effect of the complexes on the specific relative viscosity of DNA (figure 5b). The relative specific viscosity η/η_0 (η and η_0 are the specific viscosities of DNA in the presence and absence of the complexes, respectively) of DNA is a measure of the increase in contour length associated with the separation of DNA base pairs caused by intercalation. A classical DNA intercalator like ethidium bromide shows a significant increase in the viscosity of the DNA solutions. In contrast, a partially intercalated DNA complex would result in less pronounced effect on the viscosity.[54] The groove binder Hoechst 33258 was used as a reference compound that showed insignificant increase in viscosity. While the viscosity profile of the pydppz complex **2** is similar to that of EB indicating partial DNA intercalative mode of binding of the pydppz complex, the viscosity profile of the pyphen complex **1** is suggestive of DNA groove binding.[55]

3.4 *MTT Assay*

The photocytotoxicity of complexes **1** and **2** was studied in breast cancer cell line MCF-7 and keratinocyte HaCaT cells by MTT assay. The complexes upon prior

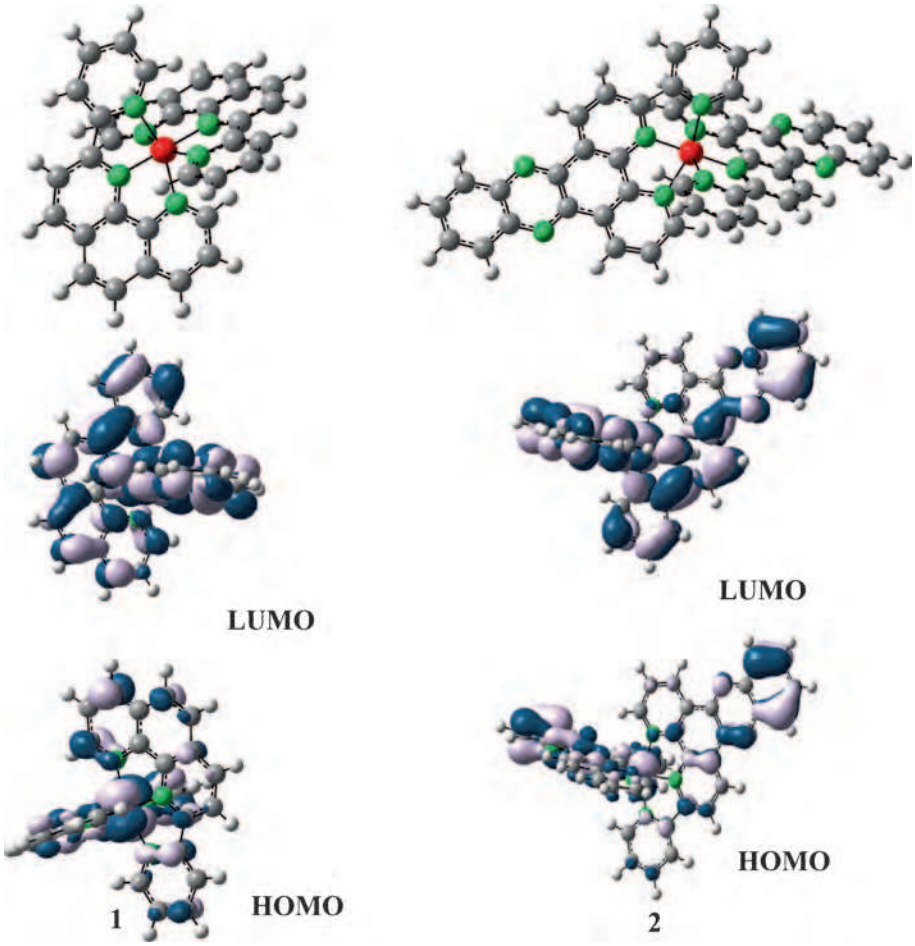

Figure 3. The energy optimized structures of complexes **1** and **2** along with the FMOs.

incubation for 4 h in dark and subsequent photoexposure to visible light of 400–700 nm for 1 h showed a dose dependent decrease in cell viability with an IC_{50} value of complex **2** being 0.08($\pm$0.01) μM for HaCaT and 13.1($\pm$1.0) μM for MCF-7 cells (figure 6). The cells unexposed to light gave an IC_{50} value of 6.8 μM for HaCaT and $>$ 100 μM for MCF-7 indicating low dark toxicity in MCF-7 cell line but moderate dark toxicity in HaCaT cell line. Complex **1** gave an IC_{50} value of 51.3($\pm$1.1) μM upon exposure to visible light of 400–700 nm and $>$ 100 μM in dark in MCF-7 cell line. Complex **2** with better photosensitizing ability showed greater photocytotoxicity in cancer cells like MCF-7 as compared to complex **1**. However, complex **2** did not show any significant photocytotoxic effect in non-cancerous cell line HaCaT.

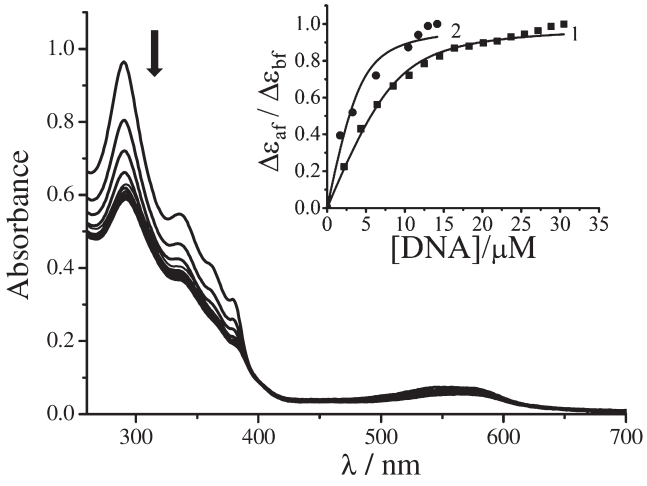

Figure 4. Absorption spectral traces of complex **2** in 5 mM Tris-HCl buffer (pH 7.2) on increasing the quantity of ct-DNA. The inset shows the MvH fitting for the complexes **1** and **2**.

3.5 *DCFDA Assay*

DCFDA assay was done to detect formation of any cellular ROS. Cell permeable DCFDA on oxidation by cellular ROS generates the fluorescent product DCF, with an emission maximum at 525 nm which can be detected by flow cytometry analysis. A substantial positive shift in the fluorescence (indicating ROS generation) was

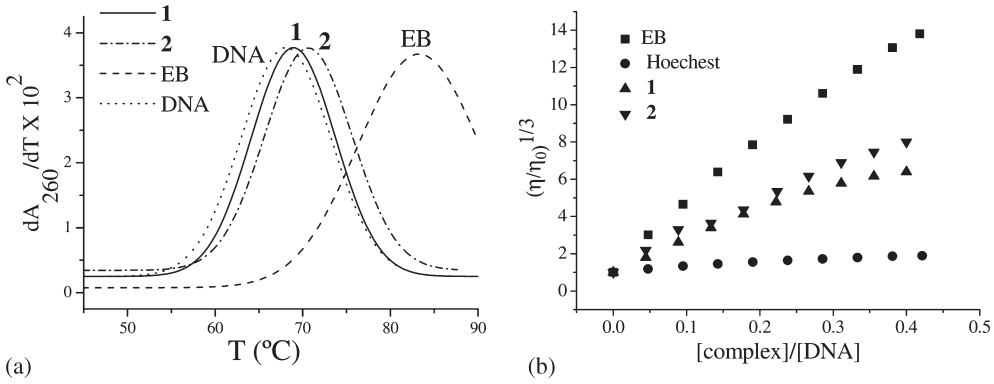

Figure 5. (a) Thermal denaturation plots of 200 μM ct-DNA alone and on addition of the complexes **1** and **2**; (b) Effect of increasing the concentration of the complexes**1**(▲),**2** (▼), ethidium bromide (EB,■) and Hoechst 33258 (●) on the relative viscosities of 150 μM ct-DNA in 5 mM Tris-HCl buffer at 37.0(±0.1) °C.

observed for MCF-7 cells treated with complexes **1** and **2** upon irradiation with visible light of 400−700 nm compared to dark and the untreated cells (figure 7a).

3.6 *Cell cycle analysis*

To examine the role of the complexes in the cell cycle, the DNA content of MCF-7 cells treated with complexes **1** and **2** was measured using a fluorescent dye, *viz.* propidium iodide (PI) by flow cytometry (figure 7b). The experiments were performed under both light and dark conditions. The complexes in dark did not induce any significant change (< 10%) in the sub-G1 population (which indicates cell death) of the cells. Complex **1** on photo-irradiation stimulated modest cell death (∼10%). However, under identical experimental conditions, complex **2** showed a marked increase in the sub-G1 population (∼25%). These data

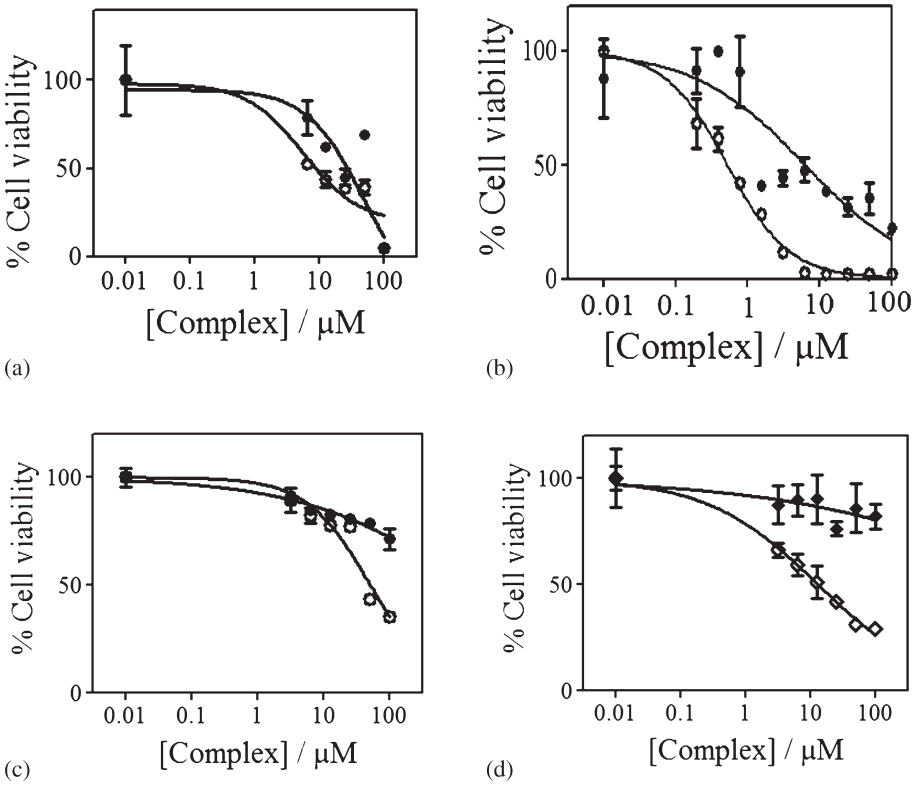

Figure 6. Photocytotoxicity of the complexes **1** and **2** in HaCaT[(a) and (b)] and in MCF-7 [(c) and (d)] cells on 4 h incubation in dark followed by exposure to light of 400–700 nm (10 J cm^{-2}).

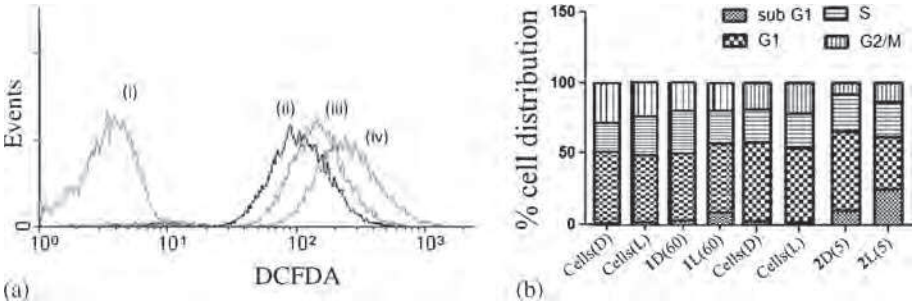

Figure 7. (a) DCFDA assay for generation of ROS in MCF7 upon exposure of visible light: (i) the fluorescence of cells alone, (ii) the fluorescence of cells + DCFDA, (iii) the fluorescence of cells + DCFDA + **2** in dark, and (iv) the fluorescence of cells + DCFDA + **2** in light. **(b)** Cell cycle profile (sub-G1, G1, S, and G2/M phases) of the MCF-7 cells treated with complexes **1** (60 μM) and **2** (5 μM) in dark and after irradiation with visible light (400−700 nm, 10 J cm^{-2}).

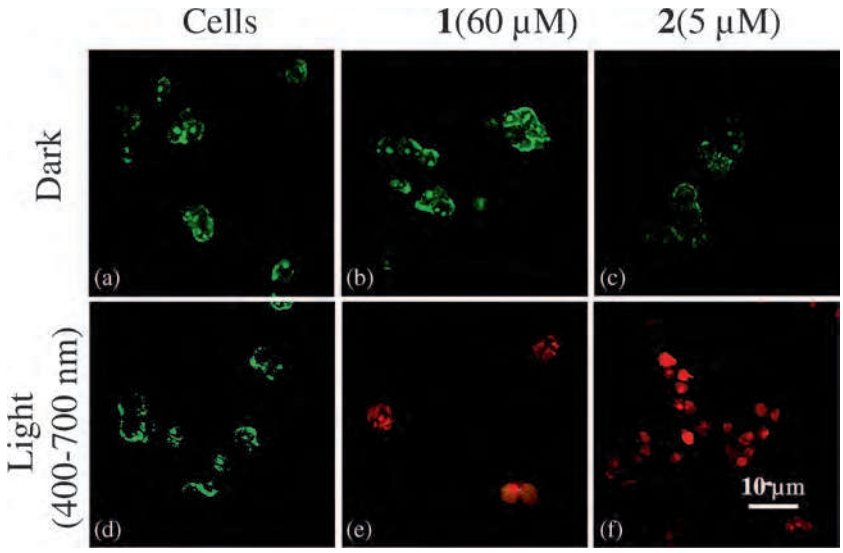

Figure 8. Confocal microscopy images of MCF-7 cell line upon AO/EB staining: panels (a) and (d) correspond to untreated cells in dark and light (400 –700 nm), panels (b) and (e) show cells treated with **1** (60 μM) in dark and light (400–700 nm) and panels (c) and (f) show cells treated with **2** (5 μM) in dark and light (400–700 nm). Scale bar corresponds to 10 μm.

are in agreement with the photocytotoxicity data of the complexes.

3.7 *Ethidium bromide/acridine orange dual staining*

EB/AO dual staining experiment was performed in MCF-7 cells using complexes **1** and **2** to further investigate their ability to induce any cell death by apoptosis. The experiment was based on the discrimination of live cells from the dead cells on the basis of membrane integrity. AO, which can pass through the plasma membrane, stains the live cells and fluoresces green. EB on the other hand is excluded from the cells having intact plasma membrane and stains only the dead cells, showing orange fluorescence. The cells incubated with the complexes **1** (60μM) and **2** (5μM) for 4 h and irradiated with visible light (400−700 nm, 10 J cm^{-2}) showed significant reddish orange emission characteristic of the apoptotic cells (figure 8). The controls incubated in dark displayed prominent green emission.

4. Conclusions

Iron(II) complex having planar pyridyldipyridophenazine base showed remarkable PDT effect in visible light with low dark toxicity in cancer cell. The pyphen and pydppz complexes are efficient binders to ct-DNA showing partial DNA intercalative binding.

The results obtained from dual staining using acridine orange and ethidium bromide suggest apoptotic mode of cell death. The results showing the low-spin diamagnetic iron(II) complexes as non-toxic in dark and significantly cytotoxic in light are of importance considering their paramagnetic iron(III) and high-spin iron(II) analogues are known to show significant dark cellular toxicity.[31]

Supplementary Information

All additional information pertaining to characterization of the complexes using ESI-MS technique (figures S1, S2), IR spectra (figures S3, S4), cyclic voltammograms (figures S5, S6), electronic spectra (figures S7, S8), TDDFT data (table S1) and atomic coordinates for the energy minimized structures (tables S2, S3) are available at www.ias.ac.in/chemsci.

Acknowledgements

We thank the Department of Science and Technology (DST), Government of India, and the Council of Scientific and Industrial Research (CSIR), New Delhi, for financial support (SR/S5/MBD-02/2007 and 01 (2559)/12/EMR-II). ARC thanks the DST for the J.C. Bose national fellowship and the Alexander von Humboldt Foundation, Germany, for donation of an electrochemical system. We thank Ms. Deepti Bapat for the confocal microscopy images, Ms. Kavya A and Mr. Vashisht K for the FACS data, Dr. Tirtha Mukherjee and Mr. ChinnaAyya Swamy P for DFT calculations.

References

1. Ethirajan M, Chen Y, Joshi P and Pandey R K 2011 *Chem. Soc. Rev.* **40** 340
2. Bonnett R 2000 In *Chemical Aspects of Photodynamic Therapy* (London: Gordon & Breach)
3. Henderson B W, Busch T M, Vaughan L A, Frawley N P, Babich D, Sosa T A, Zollo J D, Dee A S, Cooper M T, Bellnier D A, Greco W R and Oseroff A R 2000 *Cancer Res*. **60** 525
4. Dolmans D E J G J, Fukumura D and Jain R K 2003 *Nat. Rev.* **3** 380
5. Sessler J L and Miller R A 2000 *Biochem. Pharmacol.* **59** 733
6. Burrows C J and Muller J G 1998 *Chem. Rev.* **98** 1109
7. Szacilowski K, Macyk W, Drzewiecka-Matuszek A, Brindell M and Stochel G 2005 *Chem. Rev.* **105** 2647
8. Moriwaki S I, Misawa J, Yoshinari Y, Yamada I, Takigawa M and Tokura Y 2001 *Photodermatol. Photoimmunol. Photomed.* **17** 241
9. Ochsner M 1996 *J. Photochem. Photobiol. B: Biology* **32** 3
10. Crespy D, Landfester K, Schubert U S and Schiller A 2010 *Chem. Commun.* **46** 6651
11. Farrer N J, Salassa L and Sadler P J 2009 *Dalton Trans.* 10690
12. Ostrowski A D and Ford P C 2009 *Dalton Trans.* 10660
13. Ford P C 2009 *J. Am. Chem. Soc.* **131** 15963
14. Chifotides H T and Dunbar K R 2005 *Acc. Chem. Res*. **38** 146
15. Schatzschneider U 2010 *Eur. J. Inorg. Chem.* 1451
16. Gasser G, Ott I and Nolte N M 2011 *J. Med. Chem.* **54** 3
17. Boerner L J K and Zaleski J M 2005 *Curr. Opin. Chem. Biol.* **9** 135
18. Fry N L and Mascharak P K 2011 *Acc. Chem. Res.* **44** 289
19. Smith N A and Sadler P J 2013 *Philos. Trans. R. Soc. A* **371** 20120519
20. Chakravarty A R and Roy M 2012 *Prog. Inorg. Chem.* **57** 119
21. Basu U, Khan I, Hussain A, Gole B, Kondaiah P and Chakravarty A R 2014 *Inorg. Chem.* **53** 2152
22. Banerjee S, Dixit A, Shridharan R N, Karande A A and Chakravarty A R 2014 *Chem. Commun.* **50** 5590
23. Basu U, Khan I, Hussain A, Kondaiah P and Chakravarty A R 2012 *Angew. Chem. Int. Ed.* **51** 2658
24. Mackay F S, Woods J A, Heringová P, Kašpárková J, Pizarro A M, Moggach S A, Parsons S, BrabecV and Sadler P J 2007 *Proc. Natl. Acad. Sci.USA* **104** 20743
25. Kolishetti N, Dhar S, Valencia P, Lin L, Karnik R, Lippard S J, Langer R and Farokhzad O C 2010 *Proc. Natl. Acad. Sci. U. S. A.* **107** 17939
26. Dhar S, Daniel W L, Giljohann D A, Mirkin C A and Lippard S J 2009 *J. Am. Chem. Soc.* **131** 14652
27. Umezawa Y, Morishima H, Saito S, Takita T, Umezawa H, Kobayashi S, Otsuka M, Narita M and Ohno M 1980 *J. Am. Chem. Soc.* **102** 6630
28. Burger R M 1998 *Chem. Rev.* **98** 1153
29. Kraft B J and Zaleski J M 2001 *New J. Chem.* **25** 1281
30. Garai A, Basu U, Khan I, Pant I, Hussain A, Kondiah P and Chakravatry A R 2014 *Polyhedron* **73** 124
31. Wong E L M, Fang G S, Che C M and Zhu N 2005 *Chem. Commun.* 4578
32. Hertzberg R P and Dervan P B 1982 *J. Am. Chem. Soc.* **104** 313
33. Roelfes G, Lubben M, Leppard S W, Schudde E P, Hermant R M, Hage R, Wilkinson E C, Que Jr. L and Feringa B L 1997 *J. Mol. Catal. A* **117** 223
34. Loeb K E, Zaleski J M, Westre T E, Guajardo R J, Mascharak P K, Hedman B, Hodgson K O and Solomon E I 1995 *J. Am. Chem. Soc.* **117** 4545
35. Perrin D D, Armarego W L F and Perrin D R 1980 In *Purification of Laboratory Chemicals* (Pergamon Press: Oxford)
36. Dickeson J E and Summers L A 1970 *Aus. J. Chem.* **23** 1023
37. Collins J G, Sleeman A D, Aldrich-Wright J R, Greguric I and Hambley T W 1998 *Inorg. Chem.* **37** 3133
38. Amouyal E, Homsi A, Chambron J C and Sauvage J P 1990 *J. Chem. Soc. Dalton Trans*. 1841
39. Reichmann M E, Rice S A, Thomas C A and Doty P 1954 *J. Am. Chem. Soc.* **76** 3047

40. McGhee J D and von Hippel P H 1974 *J. Mol. Biol.* **86** 469
41. Carter M T, Rodriguez M and Bard A J 1989 *J. Am. Chem. Soc.* **111** 8901
42. Mosmann T 1983 *J. Immunol. Methods* **65** 55
43. Keston A S and Brandt R 1965 *Anal. Biochem.***11** 1
44. Takanashi T, Ogura Y, Taguchi H, Hashizoe M and Honda Y I 1997 *Ophthalmol. Visual. Sci.* **38** 2721
45. Toshima K, Takano R, Ozawa T and Matsumura S 2002 *Chem. Commun.* 212
46. BeckeA D 1998 *Phys. Rev. A* **38** 3098
47. BeckeA D 1993 *J. Chem. Phys.* **98** 5648
48. Lee C, Yang W and Parr R G 1988 *Phys. Rev. B* **37** 785
49. Hay P J and Wadt W R 1985 *J. Chem. Phys.* **82** 284
50. Phillips T, Haq I, Meijer A J H M, Adams H, Soutar I, Swanson L, Sykes M J and Thomas J A 2004 *Biochemistry* **43** 13657
51. (**a**) Ramakrishnan S, Suresh E, Riyasdeen A, Akbarsha M A and Palaniandavar M 2011 *Dalton Trans*. **40** 3524; (**b**) Banerjee S, Hussain A, Prasad P, Khan I, Banik B, Kondaiah P and Chakravarty A R 2012 *Eur. J. Inorg. Chem*. 3899
52. An Y, Liu S-D, Deng S-Y, Ji L-N and Mao Z-W 2006 *J. Inorg. Biochem.* **100** 1586
53. Gunther L E and Yong A S 1968 *J. Am. Chem. Soc.* **90** 7323
54. Veal J M and Rill R L 1991 *Biochemistry* **30** 1132
55. Pellegrini P P and Aldrich-Wright J R 2003 *Dalton Trans.* 176